

# Supporting Information for: Structural or population dynamics: What is revealed by the time-resolved photoelectron spectroscopy of 1,3-cyclohexadiene? A study with an ensemble density functional theory method.

Michael Filatov,<sup>\*,†</sup> Seunghoon Lee,<sup>‡</sup> Hiroya Nakata,<sup>¶</sup> and Cheol Ho Choi<sup>\*,†</sup>

<sup>†</sup>*Department of Chemistry, Kyungpook National University, Daegu 702-701, South Korea*

<sup>‡</sup>*Division of Chemistry and Chemical Engineering, California Institute of Technology, Pasadena, California 91125, USA*

<sup>¶</sup>*R & D Center Kagoshima, Kyocera, 1-4 Kokubu Yamashita-cho, Kirishima-shi, Kagoshima 899-4312, Japan*

E-mail: mike.filatov@gmail.com; cheolho.choi@gmail.com

## Contents

1	Methodology	3
2	Details of the calculations	7

<b>3</b>	<b>Fitting the TRPES intensities at eBE 5, 5.3, 8.5, and 10 eV</b>	<b>8</b>
	<b>References</b>	<b>10</b>

# 1 Methodology

The ionization energies and the respective Dyson's orbitals were calculated in this work using the EKT-SSR method<sup>1</sup> which uses the Extended Koopmans' Theorem (EKT)<sup>2,3</sup> in connection with the state-interaction state-averaged spin-restricted ensemble-referenced Kohn-Sham (SI-SA-REKS, or SSR) method.<sup>4-9</sup> The SSR method is based on ensemble density functional theory (eDFT), where ground state eDFT<sup>10-15</sup> is used to describe the non-dynamic electron correlation originating in multireference ground states of molecules and eDFT for ensembles of the ground and excited states<sup>16-19</sup> to obtain excitation energies from a variational time-independent computation.

The ensemble representation of the density and the energy of a multi-reference electronic state results in the occurrence of the fractional occupation numbers (FONs) of several frontier KS orbitals.<sup>20-22</sup> In this work, a variant of the SSR method that treats two fractionally occupied KS orbitals accommodating in total two electrons, *i.e.*, the SSR(2,2) method, is used. In the SSR(2,2) method, the ground electronic state is approximated by a perfectly spin-paired singlet (PPS) electronic configuration and the excited state by an open-shell singlet (OSS) configuration.<sup>23</sup> For both electronic configurations, the energy expression can be written as<sup>23</sup>

$$E^X = \sum_{L=1}^{L_{max}} C_L^X E[\rho_L^\alpha, \rho_L^\beta]; \quad \sum_{L=1}^{L_{max}} C_L^X = 1, \quad (\text{SI-1})$$

where  $X = PPS, OSS$  and the coefficients  $C_L^X$  depend on the fractional occupation numbers of the active orbitals. The densities of the microstates  $\rho_L^\sigma(\mathbf{r})$ , where  $\sigma = \alpha, \beta$  is the spin, are calculated using a common set of orbitals  $\varphi_q(\mathbf{r})$  and the integer and fixed occupation numbers  $n_{q,L}^\sigma$  defined for each microstate.<sup>4,8,9</sup>

$$\rho_L^\sigma(\mathbf{r}) = \sum_q^{occ} n_{q,L}^\sigma |\varphi_q(\mathbf{r})|^2 \quad (\text{SI-2})$$

For the OSS configuration, the  $C_L^{OSS}$  coefficients are fixed by spin-symmetry and, for the PPS configuration, the  $C_L^{PPS}$  coefficients are obtained by variational optimization of the respective FONs; see Refs. 4, 8, 9, and 24 for more detail.

In the case of single-state REKS method,<sup>4,5</sup> the PPS configuration alone describes the ground electronic state of a multi-reference system. In the SA-REKS method,<sup>6,8,9</sup> in accordance with the Gross-Oliveira-Kohn variational principle,<sup>16-18</sup> an ensemble of the PPS and OSS configurations

$$E^{SA-REKS} = w_{PPS} E_0^{PPS} + w_{OSS} E_1^{OSS} \quad (\text{SI-3})$$

$$w_{PPS} + w_{OSS} = 1$$

is optimized with respect to the FONs and the KS orbitals; the latter are subject to the orthonormality constraints. In Eq. (SI-3), the subscripts 0 and 1 are added to the energies of the PPS and the OSS configurations to underline that the former represents the ground electronic state and the latter represents the excited electronic state. Variational optimization of the energy (SI-3) results in a set of one-electron equations

$$f_q \hat{F}_q \varphi_q(\mathbf{r}) = \sum_p^{occ} \varphi_p(\mathbf{r}) \varepsilon_{pq} \quad (\text{SI-4})$$

where  $f_q = n_q/2$  is the average occupation number of the  $q$ -th spin-orbital,  $\varepsilon_{pq}$  are the Lagrange multipliers for the orthonormality constraints, the one-electron Fock operators  $\hat{F}_q$  are defined as

$$\hat{F}_q = \frac{1}{2f_q} \sum_L^{L_{max}} C_L^{SA} \sum_\sigma n_{q,L}^\sigma \hat{F}_L^\sigma \quad (\text{SI-5})$$

with the Fock operators  $\hat{F}_L^\sigma$  of the individual microstates given by

$$\hat{F}_L^\sigma = \hat{h} + \sum_q \sum_\sigma n_{q,L}^\sigma \int \frac{\varphi_q^*(\mathbf{r}') \varphi_q(\mathbf{r}')}{|\mathbf{r} - \mathbf{r}'|} d\mathbf{r}' + V_{xc,L}^\sigma(\mathbf{r}) \quad (\text{SI-6})$$

Eq. (SI-4) is solved by the use of the coupling operator technique,<sup>25</sup> where the matrix of the coupling operator

$$\hat{F}_{qp} = \frac{f_q \hat{F}_q - f_p \hat{F}_p}{f_q - f_p} \quad (\text{SI-7})$$

is repeatedly diagonalized until the convergence (of the energy and the density matrix) is reached. At each self-consistent field (SCF) iteration, the FONs of the active are determined by the Newton-Raphson method, see the Supporting Information to Ref. 24 for more detail.

When the orbitals and the occupation numbers are converged, the following conditions are fulfilled

$$\forall p, q; \quad \varepsilon_{pq} = \varepsilon_{qp} \quad \implies \quad \langle \varphi_p | f_q \hat{F}_q | \varphi_q \rangle = \langle \varphi_q | f_p \hat{F}_p | \varphi_p \rangle \quad (\text{SI-8})$$

for the elements of the Lagrangian matrix in Eq. (SI-4).<sup>25</sup> Note that the off-diagonal Lagrange multipliers between the orbitals with different occupations do not vanish. Hence, the Lagrange matrix in the SA-REKS one-electron equations (SI-4) does not become diagonal upon convergence and its eigenfunctions are not the canonical orbitals satisfying the

Koopmans' theorem.<sup>26</sup>

In the SSR(2,2) method,<sup>7</sup> the variational optimization of the KS orbitals and their FONs is followed by solving a simple  $2 \times 2$  secular problem

$$\begin{pmatrix} E_0^{PPS} & \Delta_{01}^{SA} \\ \Delta_{01}^{SA} & E_1^{OSS} \end{pmatrix} \begin{pmatrix} a_{00} & a_{01} \\ a_{10} & a_{11} \end{pmatrix} = \begin{pmatrix} E_0 & 0 \\ 0 & E_1 \end{pmatrix} \begin{pmatrix} a_{00} & a_{01} \\ a_{10} & a_{11} \end{pmatrix} \quad (\text{SI-9})$$

to include possible coupling between the PPS and the OSS electronic configurations. In Eq. (SI-9),  $E_0^{PPS}$  and  $E_1^{OSS}$  are the SA-REKS(2,2) energies and the interstate coupling element  $\Delta_{01}^{SA}$  is calculated using the SA-REKS(2,2) Lagrangian matrix element  $\varepsilon_{ab}^{SA}$  between the active orbitals  $\phi_a$  and  $\phi_b$  as

$$\Delta_{01}^{SA} = (\sqrt{n_a} - \sqrt{n_b}) \varepsilon_{ab}^{SA} \quad (\text{SI-10})$$

where  $n_a$  and  $n_b$  are the FONs of the active orbitals.<sup>7,9,23</sup>

The analytical energy derivatives of the SSR individual states with respect to an external perturbation  $\lambda$  (e.g., nuclear displacement)<sup>24</sup> can be represented as

$$\frac{\partial E_X}{\partial \lambda} = \text{tr} \mathbf{D}^X \mathbf{h}^\lambda - \frac{1}{2} \text{tr} \tilde{\mathbf{W}}^X \mathbf{S}^\lambda \quad (\text{SI-11a})$$

$$+ \sum_L \tilde{C}_L^X \frac{\partial E_L^{2e}}{\partial \lambda} - \sum_L C_L^{SA} \sum_\sigma \text{tr}^X \mathbf{R}_L^\sigma \mathbf{T}_L^{\sigma, \lambda(2e)}, \quad (\text{SI-11b})$$

where  $X = 0, 1$  labels the SSR state,  $\mathbf{D}^X$  is the relaxed density matrix of the state  $X$ , and  $\tilde{\mathbf{W}}^X$  is the effective Lagrangian matrix in the basis of the eigenfunctions of Eq. (SI-4)

$$\tilde{W}_{pq}^X = \sum_L \tilde{C}_L^X \left( p \epsilon_{pq}^L + q \epsilon_{pq}^L \right) - 2 \left( {}^X Q_{pq}^{(1)} + {}^X Q_{pq}^{(2)} \right), \quad (\text{SI-12})$$

where the  ${}^j \epsilon_{pq}^L$  coefficients are given by

$${}^j \epsilon_{pq}^L = \sum_\sigma \langle p | n_{j,L}^\sigma \hat{F}_L^\sigma | q \rangle. \quad (\text{SI-13})$$

In eq. (SI-11b), the terms  $E_L^{2e}$  and  $\mathbf{T}_L^{\sigma, \lambda(2e)}$  contain the derivatives of the two-electron integrals and of the exchange-correlation potential; their expressions can be found in Ref. 24. The modified ensemble weighting factors  $\tilde{C}_L^X$ , the matrices  ${}^X \mathbf{R}_L^\sigma$ ,  $\mathbf{Q}^{(1)}$ , and  $\mathbf{Q}^{(2)}$  in Eqs. (SI-11b) and (SI-12) depend on the response vector  $\mathbf{Z}$  obtained from solving the coupled-perturbed (CP) REKS equations; see Ref. 24 for detail.

In the basis of the SA-REKS eigenfunctions, the relaxed density matrix  $\mathbf{D}^X$  is given by

$$D_{qp}^X = \delta_{qp} \sum_L \tilde{C}_L^X (n_{p,L}^\alpha + n_{p,L}^\beta) - 2 Z_{qp}^X (f_p^{SA} - f_q^{SA}) \quad (\text{SI-14a})$$

$$- 4 \delta_{qb} \delta_{pa} a_{0X} a_{1X} (\sqrt{n_a} f_a^{SA} - \sqrt{n_b} f_b^{SA}), \quad (\text{SI-14b})$$

where  $Z_{ij}^X$  is the Z-vector obtained from solving the CP-REKS equations for the state  $X$  ( $= 0, 1$ ),  $a_{kj}$  are the elements of the eigenvectors of the SSR secular equation (SI-9),  $n_a$  and  $n_b$  are the FONs of the active orbitals in the PPS configuration, and  $f_j^{SA}$  are the FONs of the SA-REKS orbitals in the averaged state. The matrix  $\mathbf{D}^X$  is the proper one-electron density matrix for the SSR individual state  $X$ , as it yields the first order properties, *e.g.*, the dipole moment, by taking the trace of its product with the matrix of the respective one-electron operator.<sup>27</sup>

The matrix  $\tilde{\mathbf{W}}^X$  in Eq. (SI-11a) gives the contribution of the derivative of the orbital orthonormality constraint to the total energy gradient, *i.e.*, the Pulay term.<sup>28</sup> Hence, this matrix is the (effective) Lagrangian matrix for the individual state  $X$ . If the energy derivative in Eq. (SI-11) was calculated for a single state (*e.g.*, by setting  $w_{PPS} = 1$ ) obtained self-consistently from solving the secular equation (SI-4), then the response vector  $\mathbf{Z}$  would vanish and the relaxed density matrix in Eq. (SI-11) would become identical to the one-particle density matrix computed from the eigenfunctions of Eq. (SI-4) and the Lagrangian in Eq. (SI-11) would become identical to the Lagrangian in Eq. (SI-4); this would recover the usual analytic gradient of an energy obtained by variational optimization with respect to the orbitals under the orthonormality constraint.<sup>28</sup>

The energies of the SSR orbitals are not explicitly defined. Hence, the ionization energies for an SSR state  $X$  cannot be obtained from the application of the Koopmans' theorem.<sup>26</sup> However, the knowledge of the relaxed density matrix and the Lagrangian matrix for the state  $X$  enables computation of the ionization energies and the respective Dyson's orbitals from the application of EKT.<sup>2,3</sup> Using EKT, the ionization energies and Dyson's orbitals are obtained as the eigenvalues and the eigenfunctions of the Lagrangian matrix converted to the natural orbitals representation,<sup>2,3</sup> with the natural orbitals being the eigenfunctions of the density matrix. This can be achieved by solving a generalized eigenproblem<sup>29</sup> for the Lagrangian matrix with the density matrix used as the metric on which the eigenfunctions are normalized.<sup>30</sup> For the SSR method, this eigenproblem reads

$$\tilde{\mathbf{W}}^X \mathbf{C}^X = \mathbf{D}^X \mathbf{C}^X \boldsymbol{\varepsilon}^X, \quad (\text{SI-15})$$

where  $\boldsymbol{\varepsilon}^X$  are the (negative) ionization energies for the individual state  $X$  and  $\mathbf{C}^X$  are the respective Dyson's orbitals. The (squares of the) norms of the eigenfunctions  $\mathbf{C}^X$

$$\|\boldsymbol{\gamma}\|^2 = \text{tr}((\mathbf{C}^X)^\dagger \mathbf{D}^X (\mathbf{D}^X)^\dagger \mathbf{C}^X). \quad (\text{SI-16})$$

yield the pole strengths of the respective ionizations.<sup>30</sup> The probability of the ionization is proportional to the respective Dyson’s norm, when a transition of the ionized electron occurs into an unstructured continuum of states.<sup>31</sup>

## 2 Details of the calculations

The EKT-SSR calculations reported in the main article were carried out using a locally modified version of the GAMESS-US program.<sup>32</sup> The calculations employ the 6-31G\* basis set<sup>33</sup> and the BH&HLYP density functional.<sup>34</sup> When solving the SA-REKS SCF equations (SI-4), the value of the  $w_{PPS}$  weighting factor was set to its default value of 0.5.<sup>6</sup>

The EKT-SSR ionization energies and Dyson’s orbitals were obtained at the geometries taken from the non-adiabatic molecular dynamics (NAMMD) trajectories reported in Ref. 35. In Ref. 35, the NAMMD trajectories for the ring opening of 1,3-cyclohexadiene (CHD) were obtained using the DISH-XF (decoherence induced surface hopping from the exact factorization) trajectory surface hopping (TSH) approach<sup>36</sup> in connection with the SSR- $\omega$ PBEh method. The time step for the integration of the nuclear trajectories was set to 0.48 fs. In this work, every tenth snapshot from the nuclear trajectories was selected for the EKT-SSR calculations; *i.e.*, the time interval between the successive snapshots is 4.8 fs. This time step is shorter than the time step used typically in the acquisition of the TRPES spectra, *e.g.*, 30 fs in Ref. 37.

The PES spectra reported in the main article were calculated using Eq. (1) of the main article, where the ionization energies and the norms of the Dyson’s orbitals were calculated by Eq. (SI-15) at the geometries generated by sampling the Wigner function of a canonical ensemble of harmonic oscillators at  $T = 300\text{K}$ .<sup>38,39</sup> These geometries were obtained previously in Ref. 35 using the geometries optimized for the ground electronic states and the respective harmonic vibrational frequencies.

The TRPES spectrum of the photochemical ring opening of CHD was calculated using Eq. (2) of the main article. The intensity of the TRPES signal was calculated on a 2D grid with  $400 \times 120$  points along the electron binding energy (eBE)  $\epsilon$  and the propagation time  $t$  dimensions and spanning the intervals  $[0,20]$  eV and  $[0,576]$  fs, respectively. The values of the intensity on the 2D grid were used to plot the TRPES spectrum in the left panel of Fig. 3 of the main article.

The 2D TRPES plot in the right panel of Fig. 3 of the main article was constructed from the eBEs and the norms of the eight first Dyson’s orbitals calculated with the EKT-SSR method for the pool of geometries selected from the NAMMD trajectories. The eBEs were put in a 2D array  $\{t, IP(t)\}$ , where  $t$  is the respective propagation time, and each  $\{t, IP(t)\}$  pair in the array was weighted by the respective Dyson’s norm  $|\gamma(t)|^2$  using the “WeightedData” function of Wolfram Mathematica<sup>40</sup> package. The obtained weighted data array was visualized using the “SmoothDensityHistogram” intrinsic function of

Mathematica with bins of  $0.07 \text{ eV} \times 4.8 \text{ fs}$  to obtain the plot shown in the right panel of Fig. 3 of the main article.

### 3 Fitting the TRPES intensities at eBE 5, 5.3, 8.5, and 10 eV

The theoretical intensities of the TRPES signal estimated by Eq. (2) of the main article were fitted by the ex-Gaussian function for the eBEs of 5, 5.3, 8.5, and 10 eV; see Fig. SI-1. These eBEs were selected for comparison with the experimental TRPES results reported by Adachi et al.<sup>37</sup> In Figs. 1 and 2 of Ref. 37, the experimental TRPES intensities at the kinetic energies of photoelectrons of 8.6, 8.3, and 3.6 eV are reported. As the ionizing radiation of 13.6 eV was used by Adachi et al.,<sup>37</sup> these signals correspond to the eBEs of 5, 5.3, and 10 eV shown in Fig. SI-1. The signal at eBEs of 8.5 eV in Fig. SI-1 corresponds to the first ionization band of the ground state CHD and *cZc*- and *tZt*-HT species. This signal is reported in Fig. SI-1 for illustration of the conclusions of the main article.

The ex-Gaussian function was used in Refs. 37 and 42 to incorporate the instrument response function in the fitting of the TRPES signal intensities. The ex-Gaussian function *exG*

$$exG(x; A, B, \tau, \sigma, \mu) = A \frac{1}{\sigma \sqrt{2\pi}} \int_0^\infty e^{-y/\tau} e^{-(x-y-\mu)^2/2\sigma^2} dy + B \quad (\text{SI-17a})$$

$$= \frac{A}{2} e^{-1/\tau(x-\mu-\sigma^2/2\tau)} \left( 1 + \text{Erf} \left[ \frac{x-\mu-\sigma^2/2\tau}{\sigma\sqrt{2}} \right] \right) + B, \quad (\text{SI-17b})$$

where  $A$  and  $B$  are the amplitude and the background constant, respectively,  $\tau$  is the exponential decay parameter, and  $\sigma$  and  $\mu$  are the variance and the offset of the Gaussian distribution function, respectively, is sufficiently flexible to describe the exponential rise and fall or the exponential fall only of the target quantity. The *exG* function is used here for consistency with the work of Adachi et al.,<sup>37</sup> where the exponential decay of the TRPES intensities at several photoelectron kinetic energies was fitted with the inclusion of the finite-time instrument response.

In the left panel of Fig. SI-1, the theoretical TRPES intensities at the eBEs of 5 and 5.3 eV are shown in the interval [0,250] fs; the same interval as in Ref. 37. The exponential decay constants of  $86 \pm 44 \text{ fs}$  and  $38 \pm 17 \text{ fs}$  are comparable with the decay constants of  $70 \pm 10 \text{ fs}$  and  $60 \pm 20 \text{ fs}$  obtained by Adachi et al.<sup>37</sup> at these eBEs.

In the right panel of Fig. SI-1, the TRPES intensities at the eBEs of 8.5 and 10 eV are shown. The former signal describes the rise of the first ionization band of CHD or *cZc*-HT in the ground electronic state. The latter signal describes the time evolution of the second ionization band of *cZc*-HT. As seen in Fig. 2 of the main article, at the eBE of 10 eV the difference between the intensities of the second PES band of CHD and *cZc*-HT in the  $S_0$  state reaches substantial magnitude. The signal at this eBE (the photoelectron

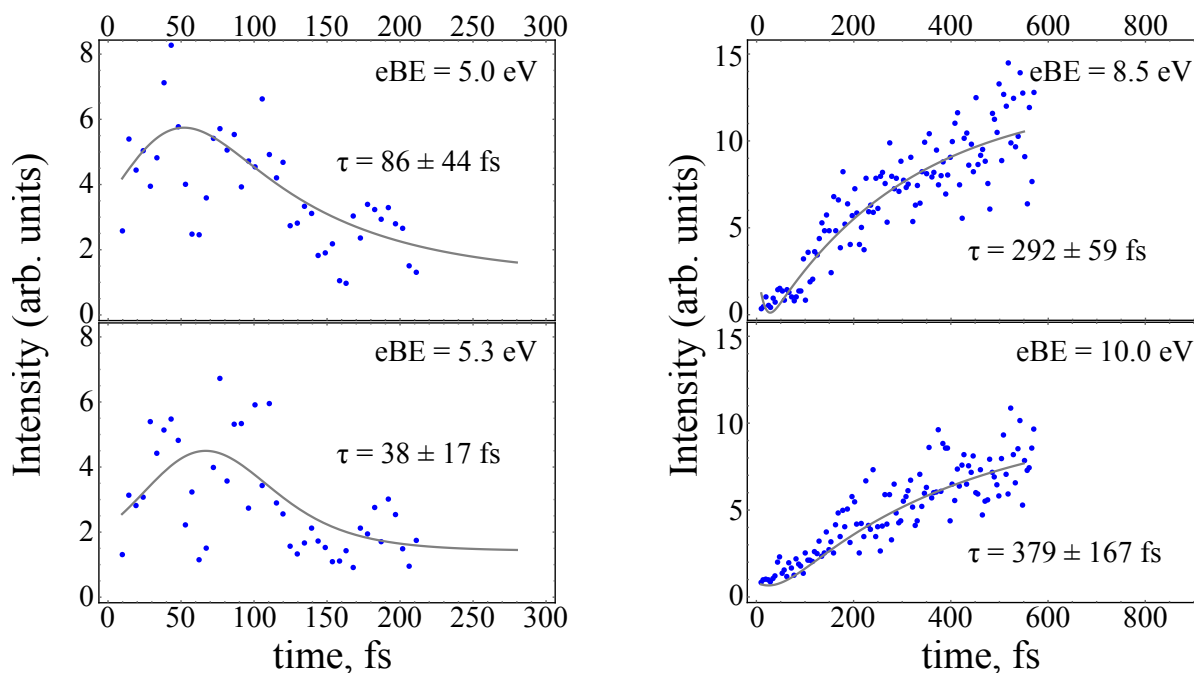


Figure SI-1: Theoretical TRPES signal intensities at the eBEs of 5.0, 5.3, 8.5, and 10 eV. The former two signals correspond to photoelectrons with the 8.6 eV and 8.3 eV kinetic energies reported in Fig. 1 of Ref. 37. The last signal (10 eV) corresponds to photoelectrons with the 3.6 eV kinetic energy shown in Fig. 3a of Ref. 37. The calculated intensities are fitted (gray solid lines) using the ex-Gaussian function; the exponential decay constants are shown in the respective plots. For the signals with the eBEs of 5 and 5.3 eV, the same intervals as in Ref. 37, *i.e.*, [0,250] fs, were used, when fitting the TRPES intensities. The margins of error were obtained by the bootstrap resampling of the fitting data.<sup>41</sup>

kinetic energy of 3.6 eV) was assigned in Ref. 37 to the recovery of the ground electronic state of the photoreaction product. The exponential decay constants of  $292 \pm 59$  fs (8.5 eV) and  $379 \pm 167$  fs (10 eV) are generally consistent with the observed kinetics of the product ground state recovery. As seen in Fig. 3a of Ref. 37, the recovery occurs on a timescale close to *ca.* 400 fs. A similar estimate for the ring opening kinetics, *i.e.*, the product formation occurs at *ca.* 400–500 fs, was obtained by Iikubo et al.<sup>42</sup> using the TRPES (29.5 eV probe) in connection with the two-photon excitation and by Kaneshima et al.<sup>43</sup> using the time-resolved high-harmonic spectroscopy.

## References

- (1) Filatov, M.; Lee, S.; Choi, C. H. Computation of molecular ionization energies using an ensemble density functional theory method. *J. Chem. Theory Comput.* **2020**, in press.
- (2) Morrell, M. M.; Parr, R. G.; Levy, M. Calculation of ionization potentials from density matrices and natural functions, and the long-range behavior of natural orbitals and electron density. *J. Chem. Phys.* **1975**, *62*, 549–554.
- (3) Smith, D. W.; Day, O. W. Extension of Koopmans' theorem. I. Derivation. *J. Chem. Phys.* **1975**, *62*, 113–114.
- (4) Filatov, M.; Shaik, S. A spin-restricted ensemble-referenced Kohn-Sham method and its application to diradicaloid situations. *Chem. Phys. Lett.* **1999**, *304*, 429–437.
- (5) Moreira, I. d. P. R.; Costa, R.; Filatov, M.; Illas, F. Restricted ensemble-referenced Kohn-Sham versus broken symmetry approaches in density functional theory: Magnetic coupling in Cu binuclear complexes. *J. Chem. Theory Comput.* **2007**, *3*, 764–774.
- (6) Kazaryan, A.; Heuver, J.; Filatov, M. Excitation Energies from Spin-Restricted Ensemble-Referenced Kohn-Sham Method: A State-Average Approach†. *J. Phys. Chem. A* **2008**, *112*, 12980–12988.
- (7) Filatov, M. Assessment of density functional methods for obtaining geometries at conical intersections in organic molecules. *J. Chem. Theory Comput.* **2013**, *9*, 4526–4541.
- (8) Filatov, M. Spin-restricted ensemble-referenced Kohn-Sham method: basic principles and application to strongly correlated ground and excited states of molecules. *WIREs Comput. Mol. Sci.* **2015**, *5*, 146–167.
- (9) Filatov, M. In *Density-functional methods for excited states*; Ferré, N., Filatov, M., Huix-Rotllant, M., Eds.; Top. Curr. Chem.; Springer: Heidelberg, 2016; Vol. 368; pp 97–124.
- (10) Valone, S. M. A one-to-one mapping between one-particle densities and some n-particle ensembles. *J. Chem. Phys.* **1980**, *73*, 4653–4655.
- (11) Lieb, E. H. Density functionals for Coulomb systems. *Int. J. Quantum Chem.* **1983**, *24*, 243–277.
- (12) Perdew, J. P.; Parr, R. G.; Levy, M.; Balduz Jr., J. L. Density-Functional Theory for Fractional Particle Number: Derivative Discontinuities of the Energy. *Phys. Rev. Lett.* **1982**, *49*, 1691–1694.

- (13) Englisch, H.; Englisch, R. Hohenberg-Kohn Theorem and Non-V-Representable Densities. *Physica* **1983**, *A121*, 253–268.
- (14) Englisch, H.; Englisch, R. Exact Density Functionals for Ground-State Energies. I. General Results. *Phys. Stat. Sol. (b)* **1984**, *123*, 711–721.
- (15) Englisch, H.; Englisch, R. Exact Density Functionals for Ground-State Energies II. Details and Remarks. *Phys. Stat. Sol. (b)* **1984**, *124*, 373–379.
- (16) Gross, E. K. U.; Oliveira, L. N.; Kohn, W. Rayleigh-Ritz variational principle for ensembles of fractionally occupied states. *Phys. Rev. A* **1988**, *37*, 2805–2808.
- (17) Gross, E. K. U.; Oliveira, L. N.; Kohn, W. Density-functional theory for ensembles of fractionally occupied states. I. Basic formalism. *Phys. Rev. A* **1988**, *37*, 2809–2820.
- (18) Oliveira, L. N.; Gross, E. K. U.; Kohn, W. Density-functional theory for ensembles of fractionally occupied states. II. Application to the He atom. *Phys. Rev. A* **1988**, *37*, 2821–2833.
- (19) Oliveira, L. N.; Gross, E. K. U.; Kohn, W. Ensemble-Density Functional Theory. *Int. J. Quantum Chem.: Quantum Chem. Symp.* **1990**, *24*, 707–716.
- (20) Schipper, P. R. T.; Gritsenko, O. V.; Baerends, E.-J. One-determinantal pure state versus ensemble Kohn-Sham solutions in the case of strong electron correlation: CH<sub>2</sub> and C<sub>2</sub>. *Theor. Chem. Acc.* **1998**, *99*, 329–343.
- (21) Schipper, P. R. T.; Gritsenko, O. V.; Baerends, E.-J. Benchmark calculations of chemical reactions in density functional theory: Comparison of the accurate Kohn-Sham solution with generalized gradient approximations for the H<sub>2</sub>+H and H<sub>2</sub>+H<sub>2</sub> reactions. *J. Chem. Phys.* **1999**, *111*, 4056–4067.
- (22) Morrison, R. C. Electron correlation and noninteracting v-representability in density functional theory: The Be isoelectronic series. *J. Chem. Phys.* **2002**, *117*, 10506–10511.
- (23) Filatov, M.; Martínez, T. J.; Kim, K. S. Using the GVB Ansatz to develop ensemble DFT method for describing multiple strongly correlated electron pairs. *Phys. Chem. Chem. Phys.* **2016**, *18*, 21040–21050.
- (24) Filatov, M.; Liu, F.; Martínez, T. J. Analytical derivatives of the individual state energies in ensemble density functional theory method. I. General formalism. *J. Chem. Phys.* **2017**, *147*, 034113.
- (25) Hirao, K.; Nakatsuji, H. General SCF operator satisfying correct variational condition. *J. Chem. Phys.* **1973**, *59*, 1457–1462.

- (26) Koopmans, T. Über die Zuordnung von Wellenfunktionen und Eigenwerten zu den Einzelnen Elektronen Eines Atoms. *Physica* **1934**, *1*, 104–113.
- (27) Perera, S. A.; Watts, J. D.; Bartlett, R. J. A theoretical study of hyperfine coupling constants. *J. Chem. Phys.* **1994**, *100*, 1425–1434.
- (28) Pulay, P. Ab initio calculation of force constants and equilibrium geometries in polyatomic molecules. *Mol. Phys.* **1969**, *17*, 197–204.
- (29) Peters, G.; Wilkinson, J. H.  $Ax = \lambda Bx$  and the Generalized Eigenproblem. *SIAM J. Num. Analysis* **1970**, *7*, 479–492.
- (30) Cioslowski, J.; Piskorz, P.; Liu, G. Ionization potentials and electron affinities from the extended Koopmans' theorem applied to energy-derivative density matrices: The EKTMPn and EKTQCISD methods. *J. Chem. Phys.* **1997**, *107*, 6804–6811.
- (31) Spanner, M.; Patchkovskii, S.; Zhou, C.; Matsika, S.; Kotur, M.; Weinacht, T. C. Dyson norms in XUV and strong-field ionization of polyatomics: Cytosine and uracil. *Phys. Rev. A* **2012**, *86*, 053406.
- (32) (a) Schmidt, M. W.; Baldridge, K. K.; Boatz, J. A.; Elbert, S. T.; Gordon, M. S.; Jensen, J. J.; Koseki, S.; Matsunaga, N.; Nguyen, K. A.; Su, S.; Windus, T. L.; Dupuis, M.; Montgomery, J. A. *J. Comput. Chem.* **1993**, *14*, 1347–1363; (b) Gordon, M.; Schmidt, M. In *Theory and Applications of Computational Chemistry, the first forty years*; Dykstra, C. E., Frenking, G., Kim, K. S., Scuseria, G. E., Eds.; Elsevier: Amsterdam, 2005; pp 1167–1189.
- (33) Krishnan, R.; Binkley, J. S.; Seeger, R.; Pople, J. A. Self-consistent molecular orbital methods. XX. A basis set for correlated wave functions. *J. Chem. Phys.* **1980**, *72*, 650–654.
- (34) (a) Becke, A. D. A New Mixing of Hartree-Fock and Local Density-Functional Theories. *J. Chem. Phys.* **1993**, *98*, 1372–1377; (b) Becke, A. D. Density-Functional Exchange-Energy Approximation with Correct Asymptotic Behavior. *Phys. Rev. A* **1988**, *38*, 3098–3100; (c) Lee, C.; Yang, W.; Parr, R. G. Development of the Colle-Salvetti Correlation-Energy Formula into a Functional of the Electron Density. *Phys. Rev. B* **1988**, *37*, 785–789.
- (35) Filatov, M.; Min, S. K.; Kim, K. S. Non-adiabatic dynamics of ring opening in cyclohexa-1,3-diene described by an ensemble density-functional theory method. *Mol. Phys.* **2019**, *117*, 1128–1141.
- (36) Ha, J.-K.; Lee, I. S.; Min, S. K. Surface Hopping Dynamics beyond Nonadiabatic Couplings for Quantum Coherence. *J. Phys. Chem. Lett.* **2018**, *9*, 1097–1104.

- (37) Adachi, S.; Sato, M.; Suzuki, T. Direct Observation of Ground-State Product Formation in a 1,3-Cyclohexadiene Ring-Opening Reaction. *J. Phys. Chem. Lett.* **2015**, *6*, 343–346.
- (38) Oppenheim, I.; Ross, J. Temperature Dependence of Distribution Functions in Quantum Statistical Mechanics. *Phys. Rev.* **1957**, *107*, 28–32.
- (39) Davies, R. W.; Davies, K. T. R. On the Wigner Distribution Function for an Oscillator. *Ann. Phys.* **1975**, *89*, 261–273.
- (40) Wolfram Research, Inc., Mathematica, Version 11.0. <https://www.wolfram.com/mathematica>, Champaign, IL, 2016.
- (41) Nangia, S.; Jasper, A. W.; Miller, T. F.; Truhlar, D. G. Army ants algorithm for rare event sampling of delocalized nonadiabatic transitions by trajectory surface hopping and the estimation of sampling errors by the bootstrap method. *J. Chem. Phys.* **2004**, *120*, 3586–3597.
- (42) Iikubo, R.; Sekikawa, T.; Harabuchi, Y.; Taketsugu, T. Structural dynamics of photochemical reactions probed by time-resolved photoelectron spectroscopy using high harmonic pulses. *Faraday Discuss.* **2016**, *194*, 147–160.
- (43) Kaneshima, K.; Ninota, Y.; Sekikawa, T. Time-resolved high-harmonic spectroscopy of ultrafast photoisomerization dynamics. *Opt. Express* **2018**, *26*, 31039–31054.